# A Hybrid MobileNet-DenseNet Model for Flood Rate Prediction

Sherubha Paul Rabin<sup>1,\*</sup>, Sasirekha Sithan Palanisamy<sup>2</sup>, Rajendran Thavasimuthu<sup>3</sup>, Amudhavalli Padmanaban<sup>4</sup>,

<sup>1\*</sup>Department of Information Technology, Karpagam College of Engineering, Coimbatore, Tamil Nadu, India.

<sup>2</sup>Department of Computer Science and Engineering, Karpagam Academy of Higher Education, Coimbatore, Tamil Nadu, India.

<sup>3</sup>Department of Sustainable Engineering, Saveetha School of Engineering, Saveetha Institute of Medical and Technical Sciences, Chennai, Tamil Nadu, India.

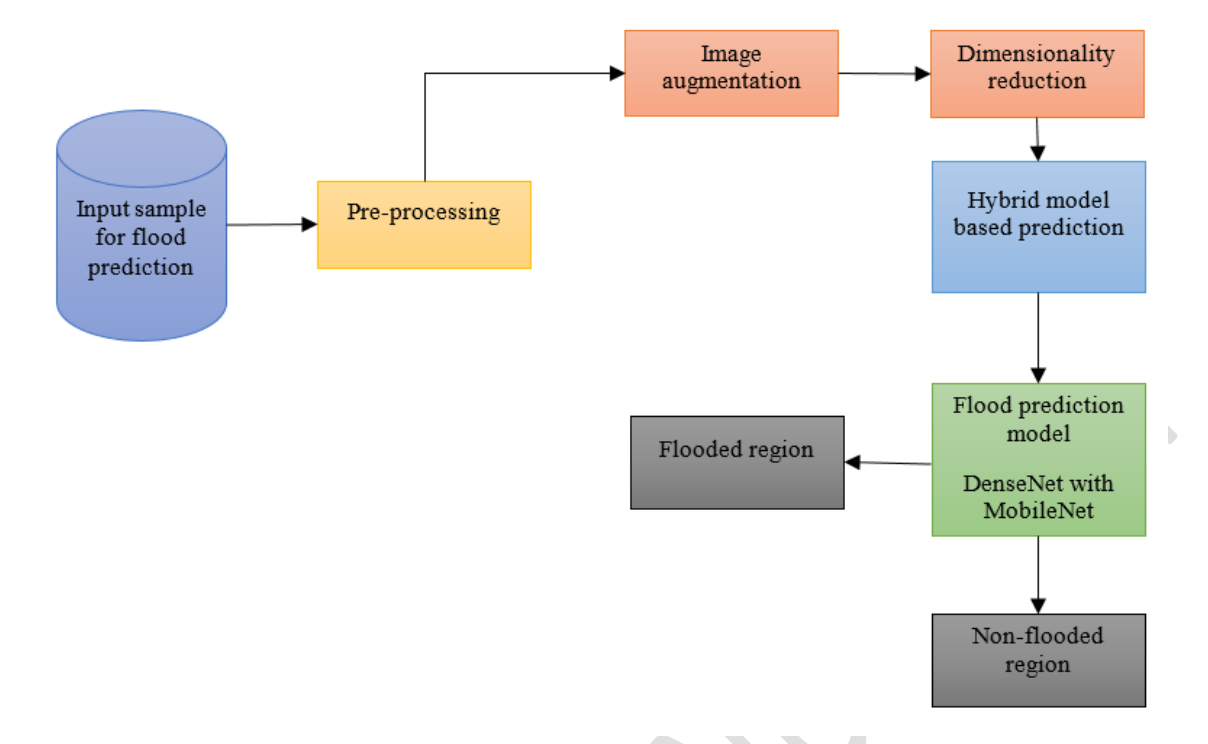
<sup>3</sup>Department of Computer Science and Engineering, JCT College of Engineering and Technology, Coimbatore, Tamil Nadu, India.

<sup>4</sup>Department of Computer Applications, School of Computer Information and Mathematical Sciences, B.S. Abdur Rahman Crescent Institute of Science and Technology, Chennai, Tamil Nadu, India.

\*Corresponding author: Sherubha Paul Rabin & Rajendran Thavasimuthu

E-mail: Sherubha0106@gmail.com & rajendran.thavasimuthusamy@ieee.org

#### **Graphical Abstract**



Abstract- Many problems arise from the increasing rain, especially in urban areas where the drainage pipeline typically cannot quickly manage large amounts of water. Flood prediction is critical for effective disaster management and mitigation, particularly in urban regions prone to severe flooding. Meanwhile, large amounts of data cannot be handled by typical flood detection models, which are unreliable for complicated processes. Deep learning (DL) approaches are frequently used in flood control to solve these issues and enhance the functionality of conventional flood detection systems. A new deep hybrid model called MobileNet-DenseNet, which uses a training method, is presented to predict floods. The filtering approach is used to pre-process the raw satellite image. Next, the weighted clustering technique divides the pre-processed image into segments. Using the retrieved feature set, a hybrid model is applied to the features to predict floods. Additionally, during the training phase, the combination data augmentation is used to choose the optimal weights for the hybrid models, thus improving their prediction performance. By adding extra neural layers to deep neural networks, this hybrid method increases their effectiveness while reducing the number of errors. The experimental findings unequivocally show that the suggested study project has met the following

analytical standards: sensitivity of 94%, specificity of 98%, accuracy of 95%, FNR of 0.02%, and FPR of 0.02%.

Keywords- Flood Prediction, Deep Learning, Prediction, Accuracy, Features.

#### 1. Introduction

One of nature's worst disasters, floods cause a great deal of death, destruction of property, and disruption of the economy. Flood occurrences are anticipated to grow more common and severe as environmental issues increase, putting people worldwide in greater danger. The need for accurate and timely flood prediction has never been more critical. Traditional flood detection systems, often reliant on statistical models and sensor networks, have demonstrated limitations in predicting flood events with the precision and speed required for effective disaster management. To reduce danger during weather events and enable remote monitoring of floods, cities must prepare flood maps (Arshad et al., 2019). However, the complexity of urban environments is such that the degree of flooding is discontinuous due to ponding, narrow, transient floods, streams at submeter resolutions, and ponding (Bai et al., 2018). It is challenging to map urban flood episodes because of these three variables. Applying methods to hydrologic systems in flood prediction is complex because of these variables (Basnyat et al., 2018).

Conventional methods are employed to map flood risk and urban flooding. Small-scale high-resolution hydrologic modeling is successful; nevertheless, acquiring the necessary computational capability with current technology is challenging. Correct assessment of the urban floods at the community level depends on precisely accurate inputs (Bochkovskiy et al., 2020). These restricting variables highlight the need for less computationally demanding mapping or forecasting methods for flooding (Bulti & Abebe, 2020; Chia et al., 2023). Over the past decade, several novel technologies have been incorporated to improve the collection of flood depth data in metropolitan settings. These technologies include object detection in flood imaging, remote sensing, DL, and social media or crowdsourced data. In the work by (Faramarzzadeh et al., 2023), the authors devised a method to differentiate between "flood" and "non-flood" events using over 100,000 online images, leveraging

artificial intelligence and content-based image retrieval. In addition, by examining text from internet news sources, the author created a DL classifier to identify flooding situations (Feng et al., 2021). Although these developments have opened up new avenues for urban flood monitoring, there is still a need for improvement in accurately and consistently monitoring floodwater levels in several locations. The utility of flood images has been enhanced by using high-resolution images from water level meters in CCTV systems to infer water levels using image recognition technology (Gauen et al., 2017).

Additionally, a low-cost, low-power cyber-physical system model detects rising water levels using a Raspberry Pi camera, image processing, and word recognition. This prototype may help a low-human-interaction flash flood detection system become widely used (Guo et al., 2021; Ichiba et al., 2018). The requirement for on-site video systems and water level meters in crowded metropolitan regions makes it difficult to install these systems in urban environments (Jiang et al., 2019; Kankanamge et al., 2020). Considering the mentioned constraints, this study attempts to provide a novel method for continuously monitoring urban flood levels at specific sites for flash floods. Traffic images during floods are analyzed using image recognition technology to assess flood levels by comparing the water surface's position relative to reference objects, such as people and vehicles.

## 1.1. Problem Statement

DL techniques have revolutionized various domains recently, offering new approaches to complex problems such as flood prediction. DL models, with their ability to learn and extract features from vast datasets, have shown promise in improving the accuracy of flood forecasts. However, these models are not without their challenges. High computing costs, overfitting, and the necessity for vast amounts of labeled data are some issues that have limited their widespread adoption in real-time flood prediction systems (Hammond et al., 2015). To address these challenges, this paper presents a new hybrid methodology for flood rate prediction and analysis, combining the strengths of two state-of-the-art DL architectures: MobileNet and DenseNet. The proposed model utilizes the lightweight and efficient nature of MobileNet, designed for mobile and embedded vision applications, and the densely

connected layers of DenseNet, known for mitigating the vanishing gradient problem and promoting feature reuse.

The paper proposes a new method for surface water depth detection in images that is more computationally and economically efficient than conventional approaches that measure flood depths using sensors and numerical models. This approach performs better when flood depth data is provided over vast areas. The proposed technology might also give real-time flood-level data by analyzing existing traffic surveillance images. Given the widespread use of traffic surveillance cameras in metropolitan areas worldwide, this method can significantly enhance urban flood monitoring and facilitate early warning systems. Remote sensing increases control over flood threats by enabling large-scale flooding without requiring incredibly accurate inputs or computationally demanding methods. Studies on predicting floods have been conducted in satellite or aerial imaging domains. No matter how much cloud cover there is, the radar is a sensor that continuously scans the surface of the Earth. Because of their shadow and latency in a complex metropolitan setting, it has been demonstrated that SAR data are unsuitable for tracking floods in metropolitan settings (Jiang et al., 2020). In real-world applications, ground truth data is scarcer; hence, unsupervised detection techniques are typically used to provide rapid flood mapping. However, with new image processing algorithms, improved data, additional information, and better processes, some progress has been made in applying SAR to applications related to urban floods. The following are this work's main contributions:

## 1.2. Research Contribution

Integrating MobileNet and DenseNet in this hybrid model creates a robust framework capable of handling the diverse and dynamic nature of flood-related data. A customized technique that maximizes the performance of both architectures is used to train the model, guaranteeing that the predictions are both accurate and computationally efficient. Because of this, the suggested model can be used in situations where prompt decision-making is necessary for efficient flood control. In this study, researchers compare the performance of the suggested hybrid model to other cutting-edge DL

methods and conventional flood prediction models. The results demonstrate that the MobileNet-DenseNet hybrid model outperforms existing methods. The successful integration of these two architectures provides a promising direction for future research in flood prediction and other environmental monitoring programs.

#### 1.3. Aim

To design an efficient and lightweight hybrid deep learning framework by integrating MobileNet and DenseNet architectures to deliver accurate real-time flood rate predictions to support proactive disaster response and reduce flood-induced damage.

# 1.4. Objectives

- ✓ To develop a hybrid deep learning model that synergizes the computational efficiency of MobileNet with the advanced feature representation capabilities of DenseNet for accurate flood rate prediction.
- ✓ Pre-processing and consolidating heterogeneous data sources—such as satellite imagery, precipitation levels, river water heights, and soil moisture—into a unified format optimized for deep learning applications.
- ✓ To assess the proposed model's performance by benchmarking it against existing approaches using key evaluation metrics, including accuracy, precision, recall, and F1-score.
- ✓ To optimize the model for real-time deployment by balancing prediction accuracy with computational efficiency, enabling effective operation on mobile or edge devices in flood-prone and resource-constrained regions.

#### 1.5. Scope

The study is centered on forecasting flood intensity—specifically the rate of water level rise—through applying deep learning techniques to environmental and meteorological datasets.

✓ It encompasses integrating data from various sources, including satellite imagery, IoT-based sensor networks, and meteorological databases.

- ✓ The hybrid model is trained and validated using historical flood records from geographically diverse regions to ensure generalizability and robustness.
- ✓ The research also explores potential real-world deployment within smart city frameworks, early warning systems, and disaster management platforms to facilitate timely and effective responses.

#### 1.6. Motivation

Floods are among the most destructive natural disasters, frequently resulting in significant loss of life, widespread property damage, and the disruption of critical infrastructure.

- ✓ Traditional hydrological models often entail intricate manual calibration and demand substantial computational resources, making them unsuitable for real-time prediction and deployment.
- ✓ In contrast, recent advancements in deep learning have shown strong capabilities in capturing spatiotemporal dependencies, essential for reliable flood forecasting.
- ✓ The proposed hybrid MobileNet-DenseNet architecture combines the lightweight efficiency of MobileNet with DenseNet's capacity for intricate feature extraction, offering a powerful solution for real-time flood prediction in resource-constrained and remote settings.
- ✓ Enhancing predictive accuracy empowers decision-makers to initiate timely interventions, thereby mitigating flood-related consequences and bolstering the resilience of vulnerable communities.

This research article is set up as follows: The analysis of the relevant literature in flood prediction using DL techniques is in Section 2. The following section details the proposed hybrid model's architecture, training methodology, and dataset used for evaluation. The experimental findings and a comparison of the model's performance with existing approaches are shown in Section 4. The work eventually ends in Section 5, which summarizes the key results and prospective avenues for additional research.

#### 2. Related works

Li et al. (2018) created a unique time series analytic processing method to determine the Mekong Delta's floodable areas using current satellite imagery. Professionals were interested in these significant issues, and researchers employed the image LiDAR/image RADAR to monitor and identify changes in floodable regions, manage flood hazards, and map flood zones. Maps, assessments, and forecasts of floods resulting from ice jams and snowmelt were conducted by Li et al. (2019) using operational meteorological satellites. When paired with temperature measurements, satellite-based flood forecasts were meant to yield more precise locations and timings of floods brought on by ice jams and snowmelt. Wide-end users could now dynamically detect and forecast floods induced by ice jams and snowmelt thanks to the efforts and outcomes of this study's flood products from VIIRS and GOES-R. The method for identifying floods in a time series was extended by (Mignot et al., 2019), and they looked at the forecasting of flood episodes by contrasting two subsequent Sentinel-2 images. Three water-sensitive satellite bands were tested as input series, and DCNN, which had been pre-trained and fine-tuned, was used to identify floods. Different remote sensing-based baseline CD techniques were used to compare the suggested strategy (Misra, 2019). More precise determination and assessment of the floods' impact was made possible by the proposed method by the crisis management authority. Using Google Earth Engine (Nigussie & Altunkaynak, 2019), an ML-based method was created to map and forecast the daily downscaling of 30-m flooding. The NOAA global prediction model's rainfall forecasts and SMAP and Landsat retrievals were combined to create and train the CART technique (Park et al., 2021; Rangari et al., 2019). When FW projections over randomly selected dates were compared against Landsat readings, an independent verification process found a significant correlation (R = 0.87). A flood segmentation method was created by (Rong et al., 2020) and was successful on the accelerator on the PhiSat-1 (Singh et al., 2018) (Wang et al., 2021), producing flood masks to be sent in place of the raw images. An effort was made to make this concept easier to illustrate by the current ESA PhiSat-1 project, which integrates a power-constrained ML accelerator, hardware capabilities for onboard processing, and wang et al. (2013); they proposed a semi-supervised learning approach with progressive accuracy gains through pseudo-labeling. A three-stage cycle approach was employed: 1) Utilizing a hand-labeled dataset with early availability and high confidence to train multiple U-Net frameworks in an ensemble method; 2) Removing poorly generated labels; and 3) Integrating the dataset with the created labels.

Urban flood forecasting utilizing machine learning (ML) and geographic information systems was proven by Wang et al. (2018). This study will integrate GIS methods and ML classifiers to develop a flood forecasting system that could be a helpful instrument for urban planning. The approach above proved beneficial in formulating a long-term strategy for smart cities, as it yielded reasonable flood risk indices and components. Random Forest was a successful ML methodology with 96% accuracy. The increased false-positive rate brought about by the increased sensitivity implies that a higher system threshold is required. The author developed two deep-learning neural network architectures in 2021 for mapping and predicting the probability of spatial floods: CNN and RNN. In the Golestan Province in northern Iran, environmental factors and historical flood disaster data were compiled into a geospatial database, which was used to create and evaluate the predictive models. Following their training using the SWARA weights, the CNN and RNN models underwent the standard procedure for validation. The outcomes demonstrated that in terms of forecasting future floods, with an AUC of 0.814 and an RMSE of 0.181, the CNN model outperformed the RNN model. They aim to simplify the complicated structure of flood disasters, yet they frequently result in inaccurate results. Sentinel-1 and Sentinel-2 employed multitemporal techniques in a CNN-based guided flood mapping demonstration (Yin et al., 2015). Introduced was OmbriaNet, which is reliant on CNN. It utilized the variations in time among flood episodes to differentiate between permanent and flooded water areas that multiple sensors can extract. This research demonstrated the process of generating a supervised

dataset using novel platforms to aid in handling flood-related emergencies. However, CNNs have

demonstrated decent performance when used for supervised categorization on a small geographic

scale. In 2022, the author examined changes in the northeastern Caspian Sea's coastline using geographic information systems (GIS) and remote sensing methods to forecast the intensity of floods caused by sea level rise. The suggested technique for making dynamic maps- utilizing GIS and remote sensing was applied to follow the shoreline and predict the amount of flooding in a specific location. Predicting when the northeast coast would flood was easy with just one map. However, the forecast quality is decreased by the constant ecological degradation and fluctuating sea level.

A DL system (CNN-LSTM) was presented by Yu et al. (2018) to analyze rainfall radar maps in two dimensions and calculate runoff directly. The CNN-LSTM model used in this study had NSE values comparable to or less than those from the previously described study. The Nash-Sutcliffe efficiency (NSE) for runoff simulation over time may be greater than 0.85 with proper training data selection. Due to its disregard for the extreme values in the one-fold training dataset, the CNN-LSTM calculated the extreme flows inaccurately. The study found that even though the satellite data has many errors, the knowledge gleaned from it typically exceeds the measurement limitations. The location of the flooded area using various remote sensing techniques and studies is also unclear due to the poor interpretation of the data. To date, various techniques have been used to assess systems based on remote sensing. Utilizing less training data, running faster, taking less time, and offering more computational efficiency make unsupervised DL systems more dependable (Zou et al., 2019). As a result, a hybrid DL model is provided for more accurate and efficient flood mapping and detection. It provides faster processing and better performance with fewer data points. In order to help other towns that are vulnerable to flooding, the suggested approach uses satellite data to detect floods and reduce the danger of flooding related to transportation projects and the expansion of urban structures. Flood prediction has been the subject of numerous studies that have used statistical and machine learning methods to increase accuracy and give real-time updates. For example, models such as Multi-Layer Perceptron (MLP), Random Forest (RF), and Convolutional Neural Networks (CNN) have demonstrated significant success. CNNs have been used with UAVs (drones) to evaluate real-time flood damage to infrastructure. In contrast, RF models have demonstrated a remarkable 98.5% accuracy in recognizing flooded areas in one instance. Furthermore, many watershed simulations have used hydrological models, like the Hydrologic Engineering Center's Hydrologic Modeling System (HEC-HMS), to forecast floods. The Tabouk watershed research demonstrates that these models mimic rainfall and runoff using information from topography, land use, soil types, and historical storm events. HEC-HMS is key in estimating peak flow rates and identifying flood-prone zones. These studies highlight the growing trend of combining machine learning with traditional hydrological models, often incorporating data from GIS, remote sensing, and UAVs to increase flood detection precision and efficacy forecasting and risk mitigation strategies (Subramanian et al., 2024; Sundarapandi et al., 2024; Venkatraman & Surendran, 2023; Venkatraman et al., 2024).

In recent years, DL models have emerged as a promising advancement offering significant improvements in prediction accuracy, scalability, and regional applicability for food forecasting (Babu et al., 2024). Several DL techniques are commonly employed in food forecasting, including convolutional neural networks (CNN) (Surendran et al., 2021), recurrent neural networks (RNN) (Arun et al., 2022), deep belief networks (DBN), long short-term memory (LSTM) (Jasmine et al., 2025), and gated recurrent units (GRU). These DL algorithms excel at handling high-dimensional and spatiotemporal data, which are critical factors in food forecasting (Nirmal et al., 2025). RNNs, in particular, have attracted significant attention due to their capacity to effectively capture sequential data through specialized recurrent hidden units (Babu et al., 2024). However, traditional RNNs face limitations such as the vanishing and exploding gradient problems, making it challenging to process long-term sequential data (Venkatraman et al., 2025). Numerous studies have shown that LSTM, an enhanced variant of RNN, outperforms in food prediction tasks (Nirmal et al., 2025). LSTM models have been applied successfully to food forecasting, yielding impressive predictive accuracy (Karthick et al., 2018). Nonetheless, there remains a lack of comparative studies examining the relative effectiveness of ML versus DL approaches in food prediction.

#### 2.1. Research Gap

The existing literature highlights significant advancements in flood prediction and analysis through various DL and ML models, including time-series analysis, satellite imagery, and GIS integration. However, these approaches exhibit limitations, such as dependency on large datasets, computational inefficiencies, and challenges in achieving accurate predictions across diverse geographic scales. While methods like CNNs, RNNs, and hybrid models like CNN-LSTM have shown promise, they often struggle with high false-positive rates, inaccurate extreme value estimation, and limited scalability. Furthermore, many models require extensive data pre-processing and face difficulties in real-time flood prediction, particularly in resource-constrained environments. These gaps highlight the need for a more robust, efficient, and scalable approach to deliver accurate flood predictions with less reliance on extensive datasets and computational resources. The proposed hybrid model, combining MobileNet and DenseNet, aims to address these gaps by providing improved prediction accuracy and better adaptability to varying data conditions, finally enhancing flood management systems.

#### 3. Proposed Methodology

The proposed research methodology focuses on developing a hybrid deep learning model combining DenseNet and MobileNet to enhance flood prediction accuracy. The process starts with the input samples, which are first put through pre-processing procedures to guarantee the consistency and quality of the data. The next step is image augmentation, which increases the dataset and improves the model's capacity to generalize in various contexts. After that, the augmented photos are divided into areas that have been flooded and those that have not, which is crucial for model training. The pre-processed data is subjected to a dimensionality reduction procedure, which helps optimize the model's efficiency and lower its computational complexity. The hybrid model then uses the reduced-dimensional data to efficiently predict flood occurrences by combining the advantages of DenseNet and MobileNet. In order to provide precise and timely flood prediction findings, the last step entails prediction modules that distinguish between flooded and non-flooded locations. This project aims to

create a technique for identifying floods in satellite photos. The suggested hybrid model's general block diagram is displayed in Fig. 1. The study's five phases include feature extraction, segmentation, pre-processing, dataset gathering, and flood prediction.

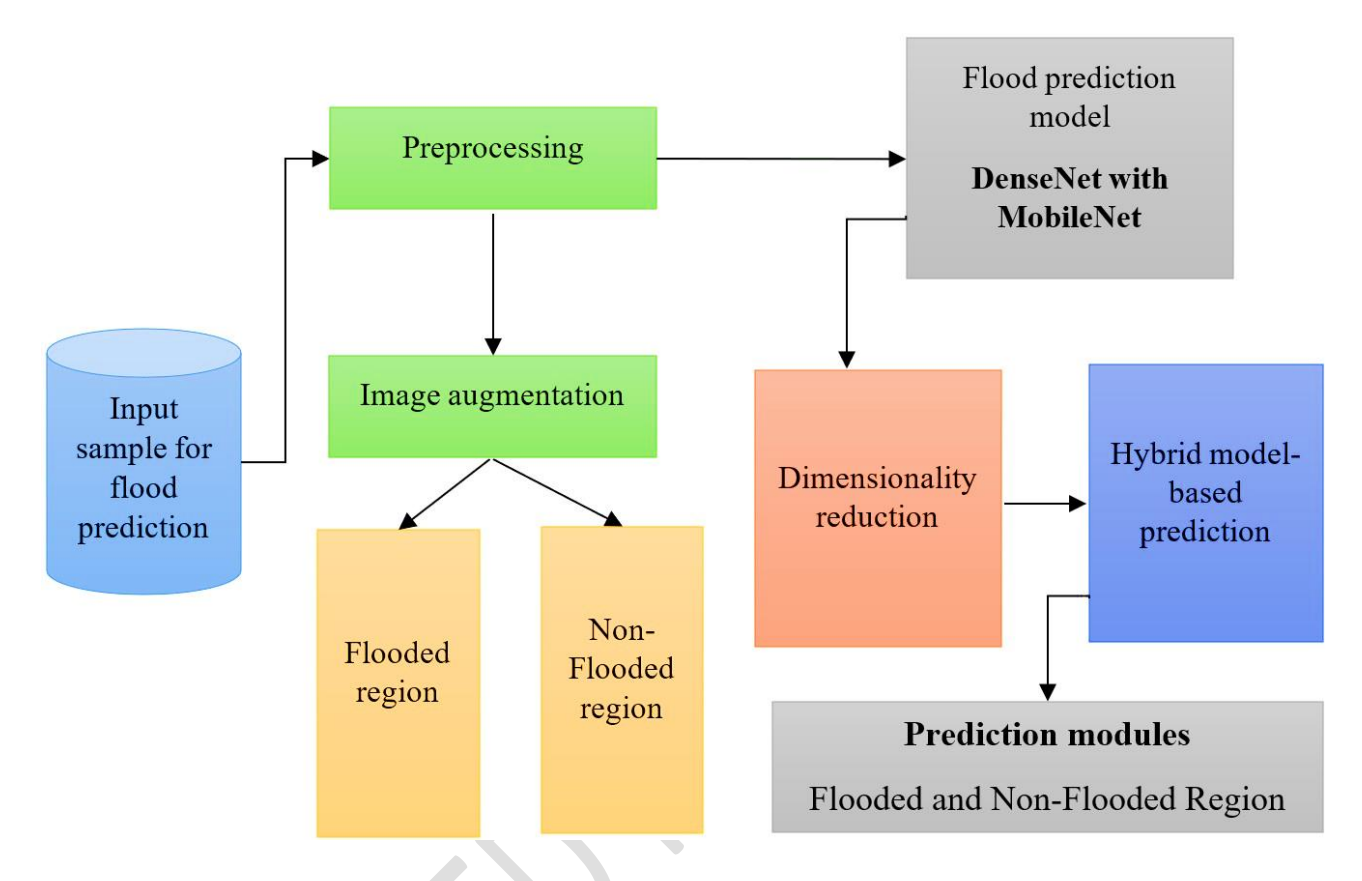


Figure 1. Workflow of the Proposed Model

#### 3.1. Details of the Dataset

Access to the data set is available at <a href="https://earthobservatory.nasa.gov/images/92669/beforeand-after-the-kerala-floods">https://earthobservatory.nasa.gov/images/92669/beforeand-after-the-kerala-floods</a>. Homes in Kerala have been destroyed by a "once-in-a-century" flood that has driven almost a million people from their homes and taken hundreds of lives. Heavy rain descended across the region on August 8, 2018. The left image was taken before the flood on February 6, 2018, using the Landsat 8 operational land imager (OLI) (bands 6-5-3). The image was taken on August 22, 2018, after the area had flooded, using the Multispectral Instrument on the Sentinel-2 satellite of the European Space Agency (bands 11–8–3). Several rivers in the region have spilled over onto the beaches.

# 3.2. Pre-processing

In this cenao, Ib  $(i,j) = b = \{1,2,...,B\}$ , where B is the number of bands, and B = 13 is the set of wavelengths that include water vapor, blue, green, red, coastal aerosol, NIR, vegetation red edge, blue, green, and red. The median filter (MF) technique is applied as a pre-processing step to the input image. MF aims to replace the value of the center pixel with the field median by analyzing the pixel sizes inside a domain. In Eq. (1), the noise is represented by r open paren i.,j close paren. The value of the final pixel determines the series' center value, filtering result  $p_b^l(i,j)$ . The sliding filter window pixels are sorted using the MF technique (Rong et al., 2020).

$$p_b^I(i,j) = median\{r(i,j), I_b(i,j) \in O_{ij}\}$$
(1)

 $O_{ij}$  Are the domain windows centered on (i,j)? The segmentation algorithm then uses the preprocessed image, designated as  $p_b^l$ , as an input; the next part goes more in-depth about this.

## 3.3. Image Augmentation

The model used picture augmentation techniques to improve its ability to overfit, extrapolate, and expand the dataset. Geometric adjustments are used to create various image sizes. The photos are rotated to 30, 60, and 90 degrees to obtain varying picture sizes. Rotating the photos by 30, 60, 90, and 120 degrees replicates patient orientation shifts. The model inverted the photos to create object variations. Elastic deformation can change the position and shape of an image-based object. Artificial samples are incorporated into state models using the superimposition technique. It aids in assessing how well the model can categorize the various labels.

The production of high-quality synthetic images is made possible by generative adversarial networks, or GANs. The system comprises two neural networks competing: a discriminant and a generator. To rectify the data imbalance, the model uses multi-channel GANs to create synthetic images. The flood photographs were used to train and evaluate the multi-channel GAN model. The images were created using pre-processed images. Without further training, pre-trained GANs enable the machine to generate flood images that resemble actual photographs. In order to do semantic interpolation, the images are also generated at many locations within the latent space (Wang et al., 2021).

$$I_i = GAN(I_i), i = 1, 2, ..., n$$
 (2)

## 3.4. Feature Representation

Using the weights from the DenseNet-121 model that was previously trained, a feature extraction model was developed. A series of convolutional layers, batch normalization, and the ReLu function are used for feature extraction. The suggested feature extraction model's design is seen in Figure 2. Using a 1×10<sup>-3</sup> learning rate, the DenseNet-121 model's weight is utilized to train the feature extraction model's final set of layers. Fewer parameters are needed for the feature extraction when using the frozen pre-trained DenseNet-121 model. At last, a fixed-size feature vector for every image is obtained by the global average pooling layer. The PET/CT image classification process uses as little computer power as possible, thanks to the feature extraction procedure (Wang et al., 2018). The mathematical representations for creating fixed-size features are presented in Eq. (3):

$$Feature = conv + ReLU + batch_{normalization}(I_i), \qquad i = 1, 2, ... n$$
 (3)

$$fixed\ size_{feature} = Global_{avg.pooling}\ 2D\ (features)$$
 (4)

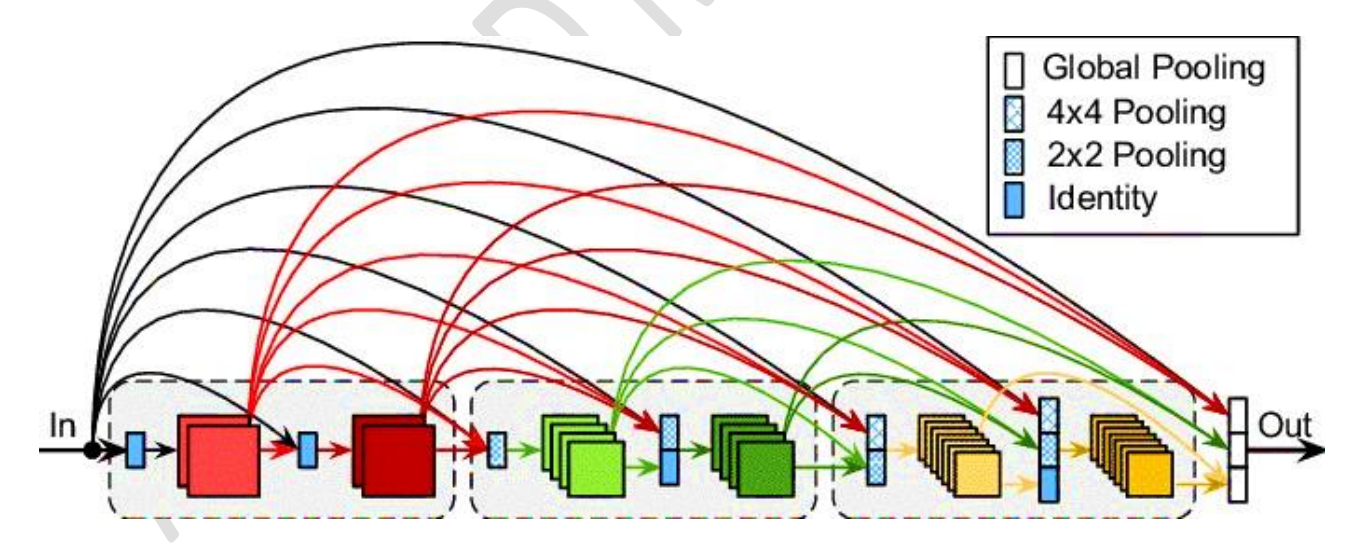


Figure 2. DenseNet Architecture for analysing the input flood samples

#### 3.5. Dimensionality Reduction

By creating a compact latent space representation, deep autoencoders are utilized to reduce the dimensionality of flood images. With the use of an encoder-decoder architecture, the goal of this

method is to use the lower-dimensional compressed representation of the input image to reproduce it. To reduce the dimensionality of the features, the model employs a multi-layer encoder network. The encoder's layers employ learned weights and biases to convert input data into a reduced-dimensional expression.

The dimensionality is decreased using various methods, such as convolutions, pooling, and non-linear activations. The provided image is subjected to latent space compression during the encoder's last stage. This latent space has considerably fewer dimensions than the initial picture. The autoencoder's design constraint is the latent space. The input image's essential components and patterns are retained in a condensed form. The decoder network aims to replicate the original feature using the low-dimensional model of the latent space. As the quantity of decoder layers increases, so do the representation's dimensions. The latent space constriction is the cause of the dimensionality reduction. The encoder network eliminates unnecessary or redundant data while maintaining the key characteristics of the features.

#### 3.6. Flood Prediction

Optimizing embedded system efficiency is MobileNet's primary goal, and MobileNet models are perfect for creating lightweight image classifiers. In contrast to larger, more parameter-heavy models, its tiny size might limit its ability to capture intricate shapes and patterns. Complex feature extraction activities, such as high-resolution image processing or sophisticated object recognition, can be beyond the capabilities of the competent MobileNet V3, as in Fig. 3. The development of MobileNet V3 models is centered on mobile devices and real-time applications. There are inevitable trade-offs between the accuracy and size of the model that need to be considered. Applications that demand precision and low processing power might not fit a MobileNet V3-Small model well. Its ability to classify flood models could be limited in terms of generality. To overcome these limitations, the research model uses the weights derived from the MobileNet V3-Small framework to develop a

classification model for image categorization. Four convolutional layers are used in total for categorization. MobileNet weights are used to train the final layers. During training, the model unblocks the three MobileNet model layers. The flood is predicted by incorporating the softmax function and fully connected layers into the model (Misra et al., 2019). The softmax function's computational version is presented in Eq. (5):

$$\sigma(\vec{\iota}) = \frac{e^{I_i}}{\sum_{j=1}^4 e^{I_j}} \tag{5}$$

The symbols represent the input vector's conventional exponential factors.  $e^{I_i}$  and  $e^{I_j}$ , respectively, and the Softmax function is symbolized by  $\sigma().\vec{i}$  Represent the image. Furthermore, by employing a decay schedule and learning rate, the model enhances training stability and convergence. Training time is reduced by optimizing the pipeline for pre-processing and data loading. The trade-off between inference performance and model size is maintained through quantization-aware training. Weight and activation redundancy in quantization-aware training maximize the research model. The final model can achieve a fourth of the initial dimensions and memory use. Additionally, accuracy is lost little to no when a factor of two to four increases inference rates. The suggested model can be utilized in real-time applications and with edge devices because of the training process. Early termination is the last tactic, shortening training time and preventing over-fitting. Flood prediction systems are frequently deployed in remote or resource-constrained environments, such as riverbanks and rural regions. Despite its compact architecture, the model incorporates squeeze-and-excitation blocks and hardswish activation functions, which significantly enhance its ability to represent features. This makes it particularly effective in extracting vital flood-related visual cues from the input frames.

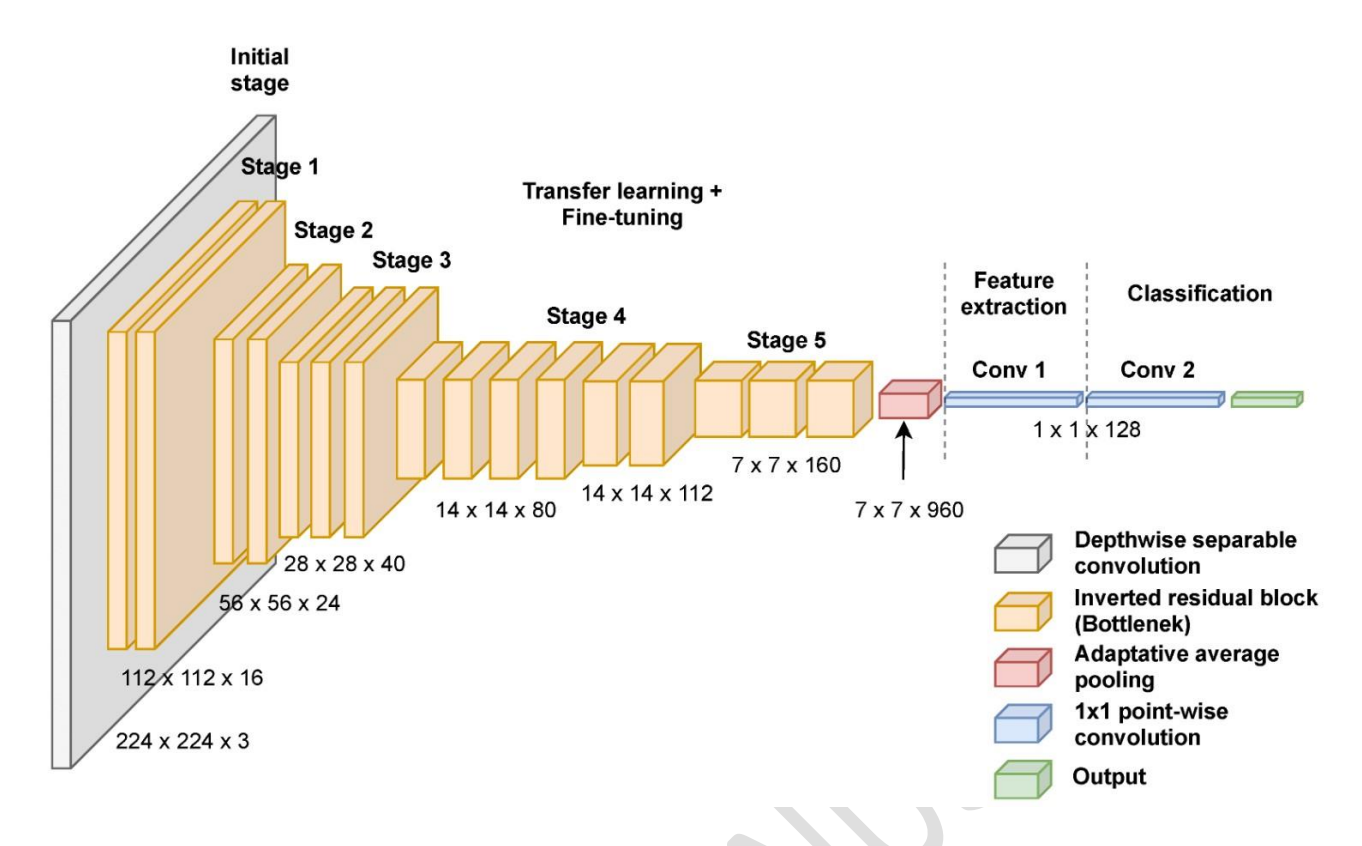


Figure 3. MobileNet Architecture for analysing the features and prediction

#### 3.7. Optimization

The proposed model utilizes the Adam (Adaptive Moment Estimation) optimizer to iteratively update its parameters during training. Adam is a sophisticated optimization algorithm that synergistically combines the strengths of two widely used methods: Adagrad and RMSProp.

- Adagrad dynamically adjusts the learning rate for each parameter by accumulating the squared gradients from previous steps, making it particularly effective for handling sparse data.
- RMSProp, in contrast, addresses Adagrad's diminishing learning rates by employing an exponential moving average of squared gradients, thereby maintaining a more stable and efficient learning process.

Adam unifies these techniques by computing and maintaining:

- The first moment (mean) of the gradients, akin to momentum, to capture the direction of the parameter updates.
- The second moment (uncentered variance), which represents the exponentially weighted average of past squared gradients, to adaptively scale the learning rates.

In the context of this model:

- The uncentered variance is dynamically updated to ensure training stability.
- The decay rates of the moving averages governed by the hyper-parameters  $\beta_1$  and  $\beta_2$ —control the influence of past gradients on current updates.
- These adaptive mechanisms enable the model to achieve faster convergence and effectively avoid local minima, which is critical for training robust flood detection systems.

Overall, this optimization strategy leverages the adaptive learning rate characteristics of Adagrad and the gradient normalization benefits of RMSProp, while Adam effectively integrates both through exponential averaging. This makes it exceptionally well-suited for complex and noisy learning environments, such as those encountered in flood prediction tasks.

#### 4. Numerical Results and Discussion

Python has been utilized in this study to accomplish the recommended flood identification in the satellite image. Operating systems: A 64-bit Intel CPU, 12 GB RAM, free disk space of 5GB, Windows 11, RHEL 6/7, Linux, and Mac OS X 10.11 are required. Multi-core CPUs, such as Intel processors, are essential for parallel processing, particularly when deploying deep learning models that require substantial computational power, such as those used in flood prediction. Systems with up to 256GB of RAM are often necessary, depending on the dataset's size and the model's complexity. This robust experimental setup allows the flood prediction system to be highly accurate, scalable, and capable of processing real-time data, which is crucial for early warning and disaster management. The subsequent experimental setups are employed (Kankanamge et al., 2020):

$$Accuracy = \frac{TP + TN}{TP + TN + FP + FN} \tag{6}$$

$$Precision = \frac{TP}{TP + FP} = 1 - FDR \tag{7}$$

$$Sensitivity = \frac{TP}{TP + FN} = 1 - FNR \tag{8}$$

$$Specificity = \frac{TN}{TN + FP} = 1 - FPR \tag{9}$$

$$FPR = \frac{FP}{FP + FN} = 1 - TNR \tag{10}$$

$$FNR = \frac{FN}{TP + FN} = 1 - TPR \tag{11}$$

$$NPV = \frac{TN}{TN + FN} = 1 - FOR \tag{12}$$

$$F - measure = \frac{2TP}{2TP + FP + FN} \tag{13}$$

$$MCC = \frac{TP * TN - FP * FN}{\sqrt{(TP + FP) + (TP + FN) + (TN + FP) + (TP + FN)}}$$
(14)

Equations (6) through (14) are used to calculate results like F-measure, specificity, sensitivity, FNR, FPR, NPV, and MCC to assess the various networks' performance. The efficacy of the deep hybrid model for flood prediction is evaluated using accuracy, NPV, FPR, and other factors, as opposed to long short-term memory (LSTM), recurrent neural networks (RNN), deep belief networks (DBN), fully convolutional neural networks (FCNN), support vector machines (SVM), and bidirectional gated recurrent units (Bi-GRU). A study on segmentation accuracy, statistical analysis, and ablation is carried out to prove the hybrid's effectiveness further. The segmented image is represented in the usual k-means algorithm. However, it cannot identify a better section for flood-affected locations since it overlaps with the existing data in various domains. The segmented image was created using one of the most popular image segmentation techniques. Also, this approach cannot discriminate between objects with comparable color intensity. This approach's accuracy is almost negligible because it initially identified the flooded area and then, over time, identified the static regions close to the flood areas. The segmented image created by the suggested hybrid approach is shown at the end. This allows for the accurate detection of the flood regions (paths) without causing any overlapping with the previously collected data. The graphic shows the afflicted area, represented by the greenish portion, and the path of flooding moving through the affected areas, represented by the orange-colored portions.

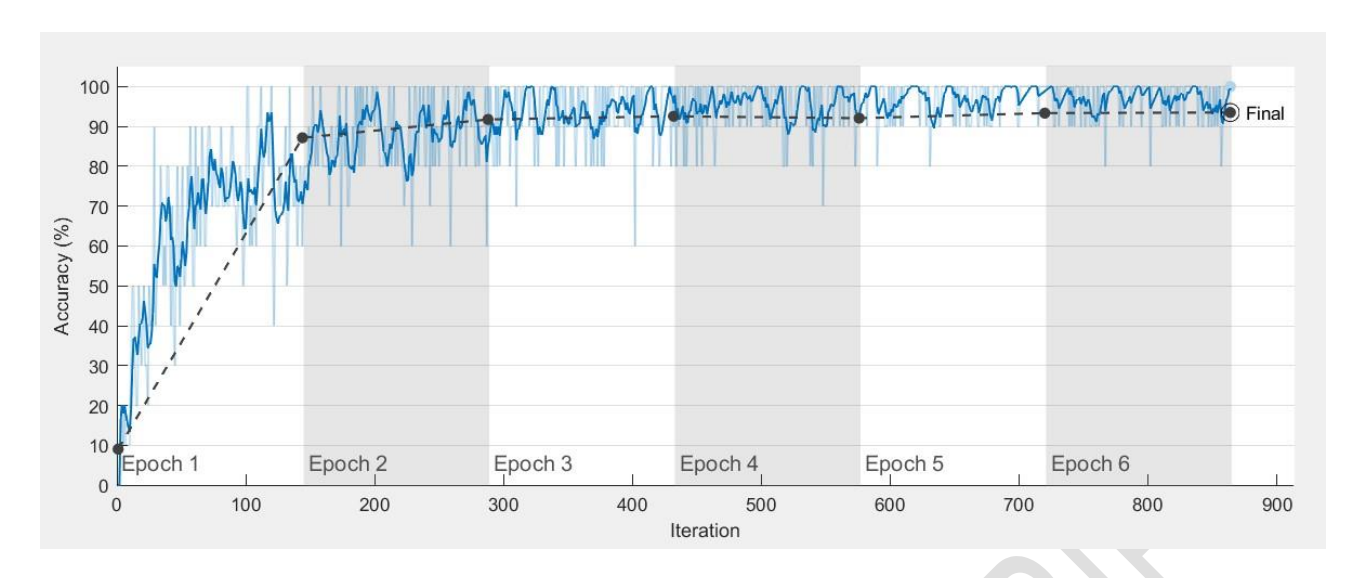


Figure 4. Training accuracy attained using MobileNet-DenseNet

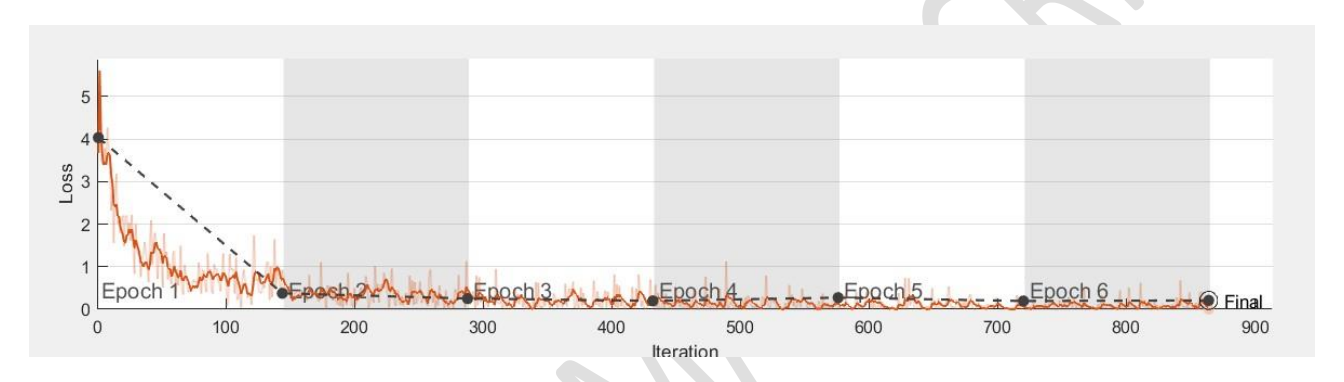


Figure 5. Training Loss attained using MobileNet-DenseNet

## 4.1. Evaluation

Table 1 compares the evaluation of the hybrid approach for detecting floods in satellite images to other metrics such as RNN, DBN, SVM, LSTM, Bi-GRU, and FCNN, as in Fig. 4 and Fig. 5. The hybrid model achieves a greater precision of about 95% at a learning rate of 80%; nevertheless, the corresponding values for RNN, DBN, SVM, LSTM, Bi-GRU, and FCNN are 79.6%, 78.1%, 78.9%, and 76%, respectively. The hybrid achieves a specificity of 98.5% when the learning is adjusted to 60%. Conversely, the other classifiers have the following specificities: SVM = 58%, Bi-GRU = 63%, RNN = 84%, DBN = 81%, LSTM = 85%, and FCNN = 65%.

The research model produced an accuracy of 95%; in contrast, the RNN, DBN, SVM, LSTM, Bi-GRU, and FCNN produced lower accuracy of 85%, 83%, 84%, 89%, 88%, 73%, 86%, 84%, 90%, 91% and 79%, respectively. At the 90th learning percentage, the proposed model reported a

sensitivity of 94%, whereas at the 70th learning percentage, it recorded a sensitivity of 81%. In addition, whereas the proposed model establishes a sensitivity of 92% at the 60th learning percentage, it maintains a sensitivity of 84% at the 80th learning percentage. The hybrid model study is computed over RNN, DBN, SVM, LSTM, Bi-GRU, and FCNN and is based on recognizing floods in satellite images. In contrast, the suggested model produced the following results at the 90% learning rate: Bi-GRU = 0.009, RNN = 0.185, SVM = 0.005, LSTM = 0.174, DBN = 0.152, and FCNN = 0.091. It also yielded an FNR of 0.02. The FPR of 0.024 was the lowest for the suggested model; however, the RNN, DBN, SVM, LSTM, Bi-GRU, and FCNN produced FPRs of 0.083, 0.094, 0.089, 0.236, 0.338, and 0.273. Consequently, the research model outperforms traditional classifiers on negative metrics, as shown in Figure 6.

**Table 1. Overall Performance Evaluation Comparison** 

Methods	Accuracy	Sensitivity	Specificity	Error rate
DBN	83.6%	85%	86%	13.56
RNN	78.8%	80%	82%	24.8
LSTM	79.8%	89%	85%	13.5
SVM	80%	90%	88%	11.6
Bi-GRU	82%	91%	88%	15.5
FCNN	81%	80%	85%	25
Proposed Hybrid Model	95%	100%	99.8%	6.50

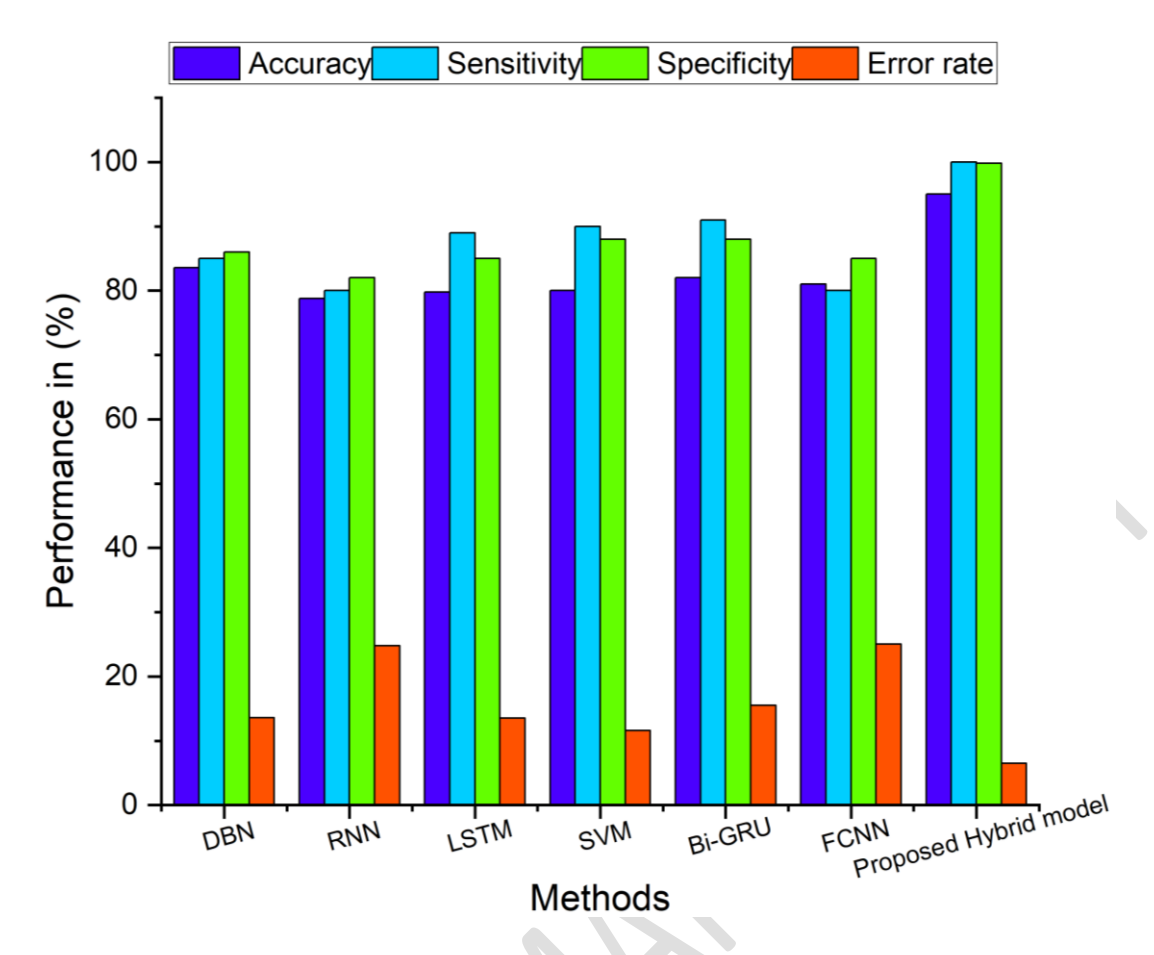


Figure 6. Overall Performance Evaluation

#### 4.2. Ablation Study

The shown model, the standard model, and the suggested model's ablation research are summarized in Table 2. The accuracy of the flood prediction with optimization, the flood forecast with the hybrid model, and the corresponding flood prediction using weighted k-means clustering and cubic chaotic map was 89.22%, 87.65%, and 93.65%. The flood prediction's FPR is 0.105 without DenseNet, 0.136 using a cubic chaotic map weighted according to k-means clustering, and 0.036 using a hybrid method. The suggested model has a 90.59% net present value, a false positive rate of 0.085797, and an accuracy of 95%, as in Fig. 7. Based on Table 2, it is proven that the proposed model with DenseNet gives promising outcomes in flood prediction compared to normal prediction strategies. The accuracy is 95%, sensitivity is 93%, precision is 93.7%, F-measure is 87%, specificity is 98%, MCC is 87% and FNR is 0.08.

Table 2. Results of the Ablation Study

Metrics	Prediction without DenseNet	Prediction with DenseNet
Sensitivity	86	93
Precision	90	93.7
F-measure	83.2	87
Specificity	89	98
MCC	85	87
Accuracy	90	95
FNR	17.2	0.08

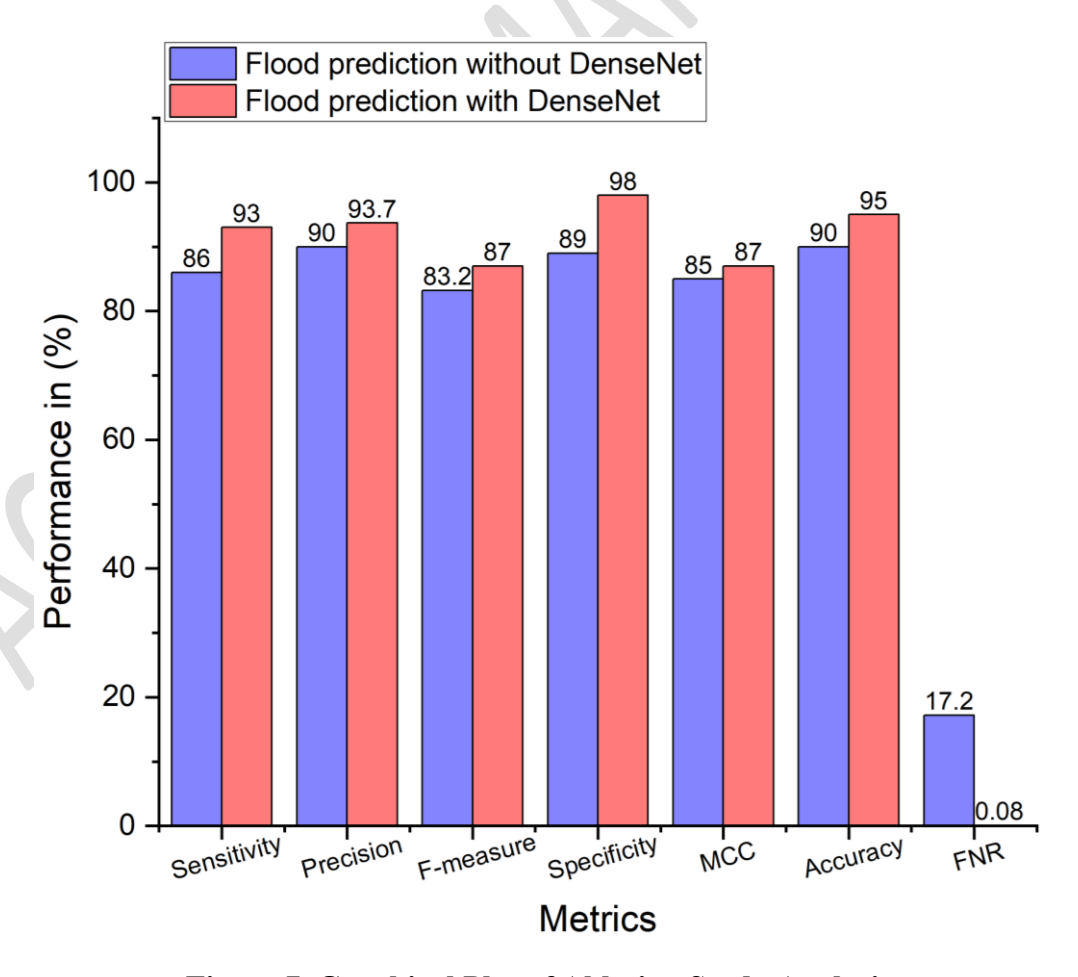


Figure 7. Graphical Plot of Ablation Study Analysis

# 4.3. Statistical Analysis

Based on five case studies, the statistical analysis examines the usefulness of suggested flood detection in satellite images, considering the mean, standard deviation, best, median, and poor values. Additionally, the proposed model is evaluated compared to RNN, LSTM, SVM, Bi-GRU, and FCNN. Table 3 presents the results. The proposed model kept its error rate at 0.034 while accounting for the best-case scenario. On the other hand, the LSTM has 0.119, the Bi-GRU has 0.144, the DBN has 0.113, the RNN has 0.132, and the FCNN has 0.226. As a result, it was demonstrated that the suggested model was appropriate for locating floods in satellite imagery.

**Table 3. Results of Statistical Analysis** 

Methods	Best	SD	Mean
DBN	0.11	0.003	0.110
RNN	0.13	0.004	0.126
LSTM	0.19	0.004	0.114
SVM	0.12	0.077	0.045
Bi-GRU	0.14	0.104	0.35
FCNN	0.22	0.022	0.175
Proposed	0.03	0.009	0.023

# 4.4. Data Convergence

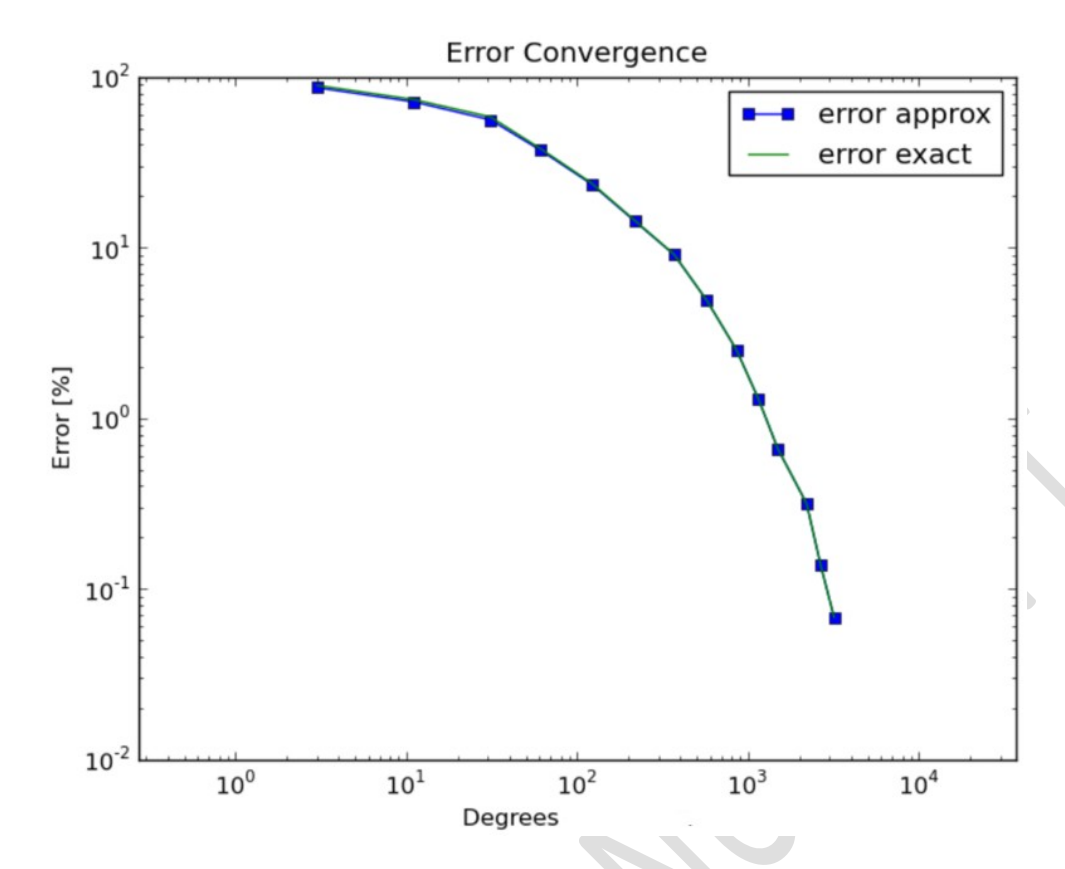


Figure 8. Error Convergence Rated based on approximation and exact outcomes

In Fig. 8, the hybrid models are contrasted with the DBN, RNN, LSTM, SVM, Bi-GRU, and FCNN to demonstrate their superiority in flood detection. The proposed model achieves a first-iteration error rate of roughly 0.45, which is lower than that of DBN and FCNN. The recommended model showed an error value of 0.63 at the 17.5th iteration; however, the current model still displayed error values of 0.21, 0.23, 0.34, 0.22, and 0.29. This demonstrates how accurate results for flood detection in satellite imagery are obtained with the proposed model. For peer review, the values of x in remote sensing were 0.34, 0.22, and 0.29, respectively. This demonstrates how accurate results for flood identification in satellite imagery are obtained with the proposed model.

# 4.5. Training and Validation Loss

The training loss ratio to validation loss ratio has grown to be the most used statistic. Validation loss indicates how well the model fits new data, while training loss indicates how well the model matches training data. Fig. 6 provides a graphic representation of the training and validation losses. The training loss started to decrease after 100 epochs, reaching a value of 0.02; in contrast, the validation loss increased to 0.05. The accuracy of recently acquired data is demonstrated by validation accuracy,

whereas training accuracy shows the correctness of previously taught data. Training and validation accuracy are graphically displayed in Fig. 6. The training accuracy begins at 0.9894, whereas the validation accuracy is 0.9813 at 100 epochs.

The proposed research model offers several key advantages, including integrating DenseNet and MobileNet, which allow for enhanced feature extraction and improved accuracy in flood prediction. Image augmentation ensures a more robust model capable of generalizing well across diverse flood scenarios. At the same time, dimensionality reduction optimizes computational efficiency, making the model faster and more resource-effective. Additionally, the hybrid approach utilized the advantages of both networks, leading to more precise and timely forecasts, which are essential for efforts to control and mitigate disasters.

Despite its strengths, the research model has some limitations. The dependence on high-quality satellite imagery and pre-processing may limit its applicability in regions with insufficient data availability or low-resolution images. The hybrid model's intricacy necessitates substantial computer resources, which would not be feasible for real-time applications in resource-constrained environments. Additionally, the input data's accuracy and quality may impact the model's performance, making it susceptible to noise or dataset abnormalities.

# 5. Conclusion

This work built a new deep hybrid flood prediction model. The augmentation strategy was used to pre-process the input satellite image. The final feature set was used for hybrid categorization. Both the deep ResNet and DenseNet classifiers received the final feature set. The outputs from both updated models were averaged to achieve the desired result. The deep ResNet and CNN weights were adjusted using the combination Adam optimizer. In addition, Adam's efficacy with the hybrid model was evaluated, and the outcomes were successfully verified. Regarding FNR, sensitivity, accuracy, and specificity, the results showed that the suggested model generated the following results: 93.48%, 98.29%, 94.98%, and 0.02% and 0.02%. A statistical analysis was carried out to find the satellite

image's mean, median, best, standard deviation, and worst values to assess the efficacy of the suggested flood identification method. The analysis's findings demonstrated that even with values for the RNN, DBN, SVM, LSTM, Bi-GRU, and FCNN, respectively, ranging from 0.113, 0.132, 0.119, 0.124, 0.144, and 0.163, the recommended model was still able to sustain an error rate of 0.034. The proposed model gives 95%, 100% sensitivity, 98.5% specificity, and a 6.50% error rate, which is substantially higher than other approaches. One of CNNs' primary features is their ability to learn directly from raw pixel input without requiring human feature engineering or pre-processing. This suggests that objects, colors, textures, shapes, and edges—among the most noticeable elements in the images are automatically identified and modified. The inference and training processes become quicker and more effective due to the input data's reduced dimensionality and complexity. Nevertheless, deep neural network design, which is strong and enables the creation of more intricate and accurate networks, has completely changed the field of computer vision science. Its poor interpretability, tendency for overfitting, and complexity are only a few of its numerous drawbacks. The suggested study can be extended to investigate more DL with more hybrid combinations of optimization approaches to overcome the restrictions and improve the accuracy of flood predictions. Large, high-quality datasets, such as historical data (river water levels and rainfall) and real-time data (such as satellite imaging and IoT sensor data), are crucial for flood prediction models. These datasets are essential for training deep learning models and producing precise and timely predictions. The efficacy of flood prediction models is hampered by the fact that such data may be lacking, insufficient, or unavailable in many rural or underdeveloped areas. Deep learning models' capacity to learn from previous flood disasters and forecast future occurrences is reduced without reliable, consistent data. More work is required to enhance data collection in these areas, either by creating techniques to deal with sparse or missing data or utilizing alternate data sources, such as crowdsourced data or mobile networks. Future studies on flood prediction can concentrate on combining deep learning architectures like Convolutional Neural Networks (CNNs) and Long Short-Term Memory (LSTM) networks with conventional machine learning models like Random Forest and XGBoost. By

integrating these methods, hybrid models can better capture flood episodes' spatial (geographical) and temporal (time-series) aspects, improving prediction accuracy overall. This technique could considerably improve real-time flood prediction skills and make them more socially beneficial, offering speedier and more accurate warnings. The model's performance may be limited by the availability and variety of high-quality training data, especially in regions with insufficient historical flood data or limited sensor infrastructure. Differences in the spatial and temporal resolutions of satellite imagery, sensor readings, and weather reports can introduce noise, potentially diminishing the model's predictive accuracy. Future advancements could include the integration of continuous real-time data streams from IoT-based flood monitoring systems to enhance responsiveness and prediction timeliness. Additionally, combining deep learning with physical hydrological models could strengthen the model's robustness by incorporating domain-specific knowledge into the prediction process. Developments in this field can be significant for enhancing flood prediction systems, supporting disaster management plans, and lowering the death toll, property damage, and displacement brought on by floods. By improving model reliability and real-time application, future research will equip authorities and communities to respond more effectively to flood hazards and limit their effects on society.

#### References

Arshad B., Ogie R., Barthelemy J., Pradhan B., Verstaevel N. & Perez P. (2019). Computer vision and IoT-based sensors in flood monitoring and mapping: A systematic review, *Sensors*, **19**(22), 5012.

Arun Mozhi Selvi Sundarapandi, Sundara Rajulu Navaneethakrishnan, Hemlathadhevi A, Surendran Rajendran\*, "A Light-weighted Dense and Tree-structured Simple Recurrent Unit (LDTSRU) for flood prediction using meteorological variables", *Global NEST Journal*. Available at: <a href="https://doi.org/10.30955/gnj.06242">https://doi.org/10.30955/gnj.06242</a>

- Babu T, Raveena Selvanarayanan, Tamilvizhi Thanarajan and Surendran Rajendran\* (2024) "Integrated Early Flood Prediction using Sentinel-2 Imagery with VANET-MARL-based Deep Neural RNN", *Global NEST Journal*, **26(10)**. https://doi.org/10.30955/gnj.06554.
- Bai Y., Zho N., Zhang R. and Zang X. (2018). Stormwater management of impacts of developments in urban areas based on SWMM, *Water*, **11**(1), 33.
- Basnyat B., Roy N. and Gangopadhay A. (2018). A flash flood categorization system uses scene-text recognition. In 2018, *IEEE International Conferences on Smart Computing (SMARTCOMP)*, 147-154.
- Bochkovskiy A., Wang C.Y. & Liao H.Y.M. (2020). Yolov4: Optimal speed and accuracy of object detections, *ArXiv Preprint ArXiv:2004.10934*.
- Bulti D.T. & Abebe B.G. (2020). A review of flood modeling methods for urban pluvial flood applications, *Modeling Earth System and Environments*, **6**, 1293–1302.
- Chia M.Y, Koo C.H, Huang Y.F, Di Chan W. and Pang J.Y. (2023). Artificial intelligence generated a synthetic dataset to remedy waters quality index estimations data scarcity, Water Resources Management, **37**(15), 6183-6198.
- Faramarzzadeh M., Ehsani M.R., Akbari M., Rahimi R., Moghaddam M., Behrangi A., Klöve B., Haghighi A.T. & Oussalah M. (2023). Applying machine learning and remote sensing for gap-filling daily precipitation data of sparsely gauged basins in East Africa, *Environmental Processes*, **10**(1), 8.
- Feng B., Zang Y. and Borke R. (2021). Urbanization impact on flood risk based on urban growth data and coupled floods model, *Natural Hazard*, **106**(1), 613-627.
- Gauen K., Dailey R., Laimann J., Ziu Y., Asokan N., Lu Y.H., Thiruvatukal G.K., Shu M.L. and Cheng S.C. (2017). Comparisons of the visual dataset for machine learning, *In 2017 IEEE International Conferences on Information Reuses and Integrations (IRI)*, 346-355.

- Guo K., Guan M. & Yu D. (2021). Urban surface water flood modeling: comprehensive reviews of current models and future challenges, *Hydrology and Earth Systems Science*, **25**(5), 2843–2860.
- Hammond M.J., Chen A.S., Djordjević S., Butler D. & Mark O. (2015). Urban floods impact assessments: A state-of-the-art review, *Urban Water Journal*, **12**(1), 14–29.
- Ichiba A., Girres A., Tchiguiriskaia I., Scherttzer D., Bommpard P. & Ten Velduis M.C. (2018). Scale effects challenge in urban hydrology is highlighted with a distributed hydrological model, *Hydrology and Earth Systems Science*, **22**(1), 331–350.
- Jasmine J, Sonia Jenifer Rayen, Ramesh T, Surendran Rajendran\* (2025) "Advanced Weather Prediction based on Hybrid Deep Gated Tobler's Hiking Neural Network and robust Feature Selection for tackling Environmental Challenges", *Global NEST Journal*, **27(4)**. https://doi.org/10.30955/gnj.06757.
- Jiang J., Liu J., Cheng C., Huang J. & Xue A. (2019). Automatic estimations of urban waterlogging depth from video image based on ubiquitous referenced object, *Remote Sensing*, **11**(5), 587.
- Jiang J., Qin C.Z., Yu J., Cheng C., Liu J. & Huang J. (2020). Obtaining urban waterlogging depth from video image using synthetic image data, *Remote Sensing*, **12**(6), 1014.
- Kankanamge N., Yigitcanllar T., Goonetileke A. and Kamruzaman M. (2020). Determining disaster severity through social media analysis: Testing the methodology with South East Queensland Flood tweets, *International Journal of Disaster Risk Reduction*, **42**, 101360.
- Karthik .S, Surendran .R\*, Sam Kumar G.V, Senduru Srinivasulu (2025) "Flood Prediction in Chennai based on Extended Elman Spiking Neural Network using a Robust Chaotic Artificial Hummingbird optimizer", *Global NEST Journal*, **27(4).** Available at: https://doi.org/10.30955/gnj.07113.
- Li J., Zhang B., Mu C. & Chen L. (2018). Simulations of a sponge city's hydrological and environmental effect based on MIKE FLOOD, *Environmental Earth Science*, 77, 1-16.

- Li Y., Martinis S. and Wieland M. (2019). Urban floods mapping with an active self-learning convolution neural network based on TerraSAR-X intensity and interferometric coherences, *ISPRS Journal of Photogrammetry and Remote Sensing*, **152**, 178-191.
- Mignot E., Li X. & Dewals B. (2019). Experimental modeling of urban flooding: A review, *Journal* of Hydrology, **568**, 334-342.
- Misra D. (2019). Mish: A self-regularized non-monotonic neural activation function, *Arxiv Preprint*Arxiv: 1908.08681.
- Nigussie T.A. and Altunkaynak A. (2019). Modeling the effects of urbanization on flood risks in Ayamama Watershed, Istanbul, Turkey, using the MIKE 21 FM model, *Natural Hazards*, **99**, 1031-1047.
- Nirmal Kumar, M., Subramanian, P., & Surendran, R. (2025). "Multivariate time series weather forecasting model using integrated secondary decomposition and Self-Attentive spatio-temporal learning network", *Global NEST Journal*, **27(4).** https://doi.org/10.30955/gnj.06195.
- Park S., Baek F., John J. & Kimm H. (2021). Computer vision–based estimations of flood depths in flooded vehicle images, *Journal of Computing in Civil Engineering*, **35**(2), 04020072.
- Rangari V.A., Umammahesh N.V. & Bhat C.M. (2019). Assessments of inundation risks in urban flood using HEC RAS 2D, *Modeling Earth System and Environments*, **5**(4), 1839-1851.
- Rong Y., Zhang T., Zheng Y., Hu C., Peng L. and Feng P. (2020). Three-dimensional urban flood inundation simulations based on digital aerial photogrammetry, *Journal of Hydrology*, **584**, 124308.
- Singh P., Sinha V.S.P., Vijahani A. & Pahja N. (2018). Vulnerability assessments of urban road networks from urban floods, *International Journal of Disaster Risk Reductions*, **28**, 237–250.

- Subramanian, S. et al. (2024). "An Automatic Data-Driven Long-term Rainfall Prediction using Humboldt Squid Optimized Convolutional Residual Attentive Gated Circulation Model in India," Global NEST Journal, **26**(10).
- Sundarapandi, A.M.S., et al. (2024). "A Light-weighted Dense and Tree-structured, simple recurrent unit (LDTSRU) for flood prediction using meteorological variables," Global NEST Journal, **26**(8).
- Surendran R\*, Tamilvizhi T, Lakshmi S, "Integrating the Meteorological Data for Smart City using Cloud of Things (CoT)", London Metropolitan University, London, United Kingdom, *Springer Nature LNICST*, **18(19)** Aug 2021.
- Venkatraman M & Surendran R (2023). "Aquaponics and Smart Hydroponics Systems Water Recirculation Using Machine Learning", 2023 4th International Conference on Smart Electronics and Communication (ICOSEC), Trichy, India, 998–1004.
- Venkatraman, M. et al. (2024). "Water quality prediction and classification using Attention-based Deep Differential RecurFlowNet with Logistic Giant Armadillo Optimization," Global NEST Journal [Preprint].
- Venkatraman, M., Surendran R \*., Senduru Srinivasulu, Vijayakumar K. (2025) "Water quality prediction and classification using Attention-based Deep Differential RecurFlowNet with Logistic Giant Armadillo Optimization", *Global NEST Journal*. https://doi.org/10.30955/gnj.0679.
- Wang C.Y., Bochkovskiy A. & Lio H.Y.M. (2021). Scaled-yolov4: Scaling cross-stages partial networks, *In Proceedings of the IEEE/CVF Conferences on Computer Vision and Pattern Recognition*, 13029-130.
- Wang X., Yan M., Zhu S. & Lin Y. (2013). Regions for generic object detections, *In Proceedings of the IEEE International Conferences on Computer Vision*, 17-24.

- Wang Y., Chen A.S., Fu G., Djordjević S., Zhang C. & Savić D.A. (2018). An integrated high-resolution urban flood modeling framework considering multiple information sources and urban features, *Environmental Modelling & Software*, **107**, 85–95.
- Yin J., Ye M., Yin Z. and Xu S. (2015). A review of advances in urban flood risk analysis over China, Stochastic Environmental Research and Risk Assessments, 29, 1063-1070.
- Yu H., Zhao Y., Fu Y. & Li L. (2018). Spatiotemporal variances assessments of urban rainstorms waterlogging affected by impervious surface expansions: A Guangzhou, China case study. Sustainability, **10**(10), 3761.
- Zou Z., Shi Z., Guo Y. and Ye J. (2019). Object detection in 20 years: A survey, *ArXiv Preprint*ArXiv:1905.05055.
- https://earthobservatory.nasa.gov/images/92669/beforeand-after-the-kerala-floods (accessed on 01/08/2025)